Structures and Excited States of Extended and Folded Mono-, Di-, and Tri-*N*-Arylbenzamides†

Frederick D. Lewis,* Timothy M. Long, Charlotte L. Stern, and Weizhong Liu

Department of Chemistry, Northwestern University, Evanston, Illinois 60208-3113

Received: July 10, 2002; In Final Form: August 21, 2002

The relationship between molecular structure and electronic properties of 18 *N*-arylbenzamides has been investigated. The secondary amides adopt extended trans-amide conformations, whereas the tertiary amides adopt folded cis-amide conformations in which the *N*-aryl group is approximately perpendicular to the benzoyl group. The *N*-aryl groups of the tertiary di- and triamides occupy the same face of the benzoyl group and display edge-to-face aryl−aryl interactions. The long-wavelength absorption maxima of the secondary amides are red-shifted as the number of *N*-aryl groups increases, whereas the tertiary amides display are blue-shifted. ZINDO calculations aid in the assignment of the absorption and luminescence spectra. In all cases the lowest energy singlet state is assigned to a forbidden n,B* (carbonyl lone-pair to benzoyl) transition. The structureless fluorescence of the secondary and tertiary amides is assigned to planar and twisted n,B* singlets, respectively. The allowed absorption bands are assigned to A,B* (arene-to-benzoyl) or A,A* (arene-to-arene) transitions which are localized on a single arene, and the structured phosphorescence is assigned to A,A* triplet states.

Introduction

Benzanilide adopts extended trans conformations both in solution and in the solid state, whereas *N*-methylbenzanilide adopts folded cis conformations.[1,2] We recently investigated the spectroscopic properties of these molecules and several other secondary and tertiary benzanilides.[3−5] In rigid media, conformational differences result in different fluorescence maxima for the secondary and tertiary benzanilide; however both form relaxed twisted singlet states with similar fluorescence maxima in fluid solution. Azumaya and co-workers[6−8] reported that the conformational preference observed for the benzanilides is conserved in the corresponding secondary and tertiary 1,3-dicarboxamides and 1,3,5-tricarboxamides. Moreover, in the solid state the tertiary di- and tri-carboxamides adopt syn conformations in which the anilide groups are located on the same side of the central ring with an edge-to-face arrangement of their phenyl groups. The syn conformation of the diamide also predominates in solution, however, the all-syn conformation of the triamide is in equilibrium with the syn−anti conformation in solution. From the temperature dependence of the ^{1}H NMR spectrum of the triamide, the all-syn conformation was found to be favored enthalpicly but disfavored entropicly ($\Delta H° = 2.1$ kcal/mol; $\Delta S° = 8.4$ cal/mol K).[8]

The conformational preferences of the secondary and tertiary di- and triamides present a unique opportunity to investigate electronic interactions in complex molecules with well-defined extended and folded geometries. To our knowledge, the only extended 1,3- and 1,3,5-trisubstituted benzene derivatives whose electronic spectra have been studied to date are the parent *meta*-terphenyl and 1,3,5-triphenylbenzene and several of their derivatives.[9−11] The electronic interactions between syn aryl groups in folded 1,3- and 1,3,5-trisubstituted benzene derivatives have not been investigated. We report here the synthesis, molecular conformation, and electronic spectra of the 18 secondary and tertiary mono-, di-, and triamides whose two-dimensional chemical structures are shown in Chart 1.[12] These amides are identified using a code in which the first number designates the order of the amide (2 = secondary; 3= tertiary), the letter R designates the identity of the aryl group (*P* = phenyl, BP = biphenyl, and DPA = diphenylacetylene), and the second number designates the number of amide substituents. All three aryl groups are derived from axially symmetric amines, thus limiting the conformational heterogeneity of the di- and triamides.

Experimental Section

General Methods. ^{1}H NMR spectra were measured on a Varian INOVA-500 MHz NMR spectrometer. UV−vis spectra were measured on a Hewlett-Packard 8452A diode array spectrometer using a 1 cm path length quartz cell. Total emission spectra were measured on a SPEX Fluoromax spectrometer. Low-temperature spectra were measured either in a Suprasil quartz EPR tube (3.3 mm i.d.) using a quartz liquid nitrogen coldfinger dewar at 77K or in an Oxford Cryogenics DN1704 cryostat fitted with an Oxford Instruments ITC4 temperature controller. Total emission quantum yields were measured by comparison to an external standard, 9,10-diphenyl anthracene ($\Phi_f \sim 1.0$ at 77K in MTHF),[13] using the integrated area under the total emission curves at equal absorbency and the same excitation wavelength. The overlapping fluorescence and phosphorescence spectra were resolved by time dependent integration as described previously.[5] All emission spectra are uncorrected, and the estimated error for the quantum yields is ±20%.

Fluorescence decays were measured on a Photon Technologies International (PTI) Timemaster stroboscopic detection instrument with a gated hydrogen or nitrogen lamp using a scatter solution to profile the instrument response function. Phosphorescence decays were measured on a PTI Timemaster phosphorescence-time-based detection instrument using a Xenon-flash lamp as the excitation source. Nonlinear least-squares fitting of the decay curves employed the Levenburg−Marquardt algorithm as described by James et al.[14] and implemented by the PTI Timemaster (version 1.2) software. Goodness of fit was determined by judging the χ^2 (<1.3 in all cases), the residuals,

† Part of the special issue "George S. Hammond & Michael Kasha Festschrift".

* Address correspondence to this author. E-mail: lewis@chem.northwestern.edu.

10.1021/jp0264937 CCC: $25.00
Published on Web 10/31/2002

CHART 1: Structures of Secondary and Tertiary Mono-, Di-, and Tribenzamides. R = −H (P), R = −Ph (BP), and R = −C≡CPh (DPA).

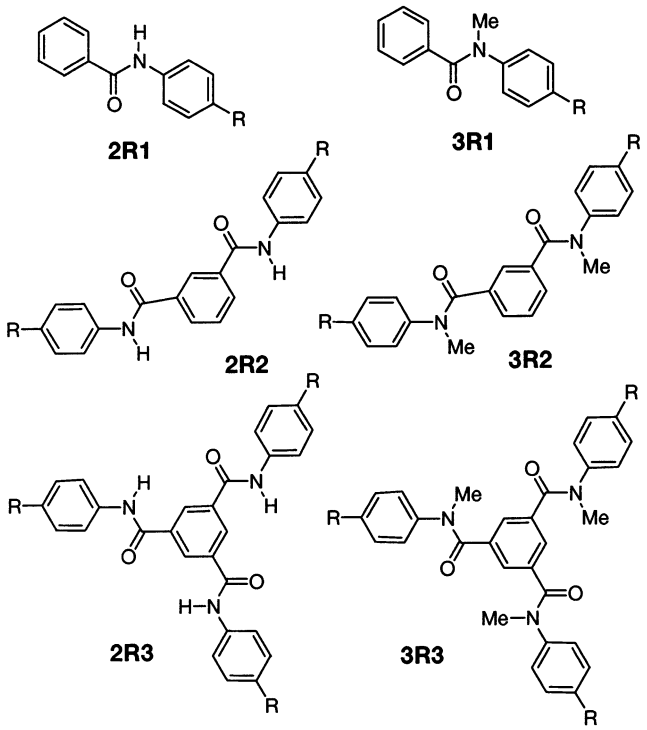

and the Durbin−Watson parameter (>1.6 in all cases). Solutions were degassed under vacuum (<0.1 Torr) through five freeze−pump−thaw cycles.

A single crystal of **3BP3** ($C_{48}H_{39}N_3O_3$, FW 705.86) was grown from toluene. A colorless prismatic crystal having dimensions 0.34 × 0.33 × 0.19 mm^3 was mounted on a glass fiber, and data for its X-ray structure collected at −120 °C on an Enraf-Nonius CAD4 diffractometer with graphite monochromated Mo Kα radiation (λ = 0.71069 Å). The crystal system is trigonal, the space group *P*3(no. 143), lattice parameters a = 16.425(4) Å, c = 12.086(2) Å: Z = 3, R = 0.104, R_w = 0.072, and GOF = 3.06.

ZINDO (INDO/S SCF-CI) calculations were performed using Cache Release 4.4 with ground-state structures optimized with AM1 method using MOPAC programs.

Materials. Benzoyl chloride, isophthaloyl dichloride, 1,3,5-benzenetricarbonyl trichloride, aniline, 4-biphenylamine, and iodomethane are commercially available and used as received. 4-Aminodiphenylacetylene was prepared from 4-iodoaniline and cuprous 4-phenylactylide as previously reported.[4] Benzanilide (**2P1**) was recrystallized from DMF and water (1:1) two times. *N*-Methyl benzanilide (**3P1**, Aldrich) was recrystallized from acetone and hexane (1:1) two times. Anhydrous MTHF containing 200 ppm BHT (Aldrich) was distilled over sodium under a nitrogen atmosphere.

General Procedure for Preparing Secondary Benzamides. To a solution of arylamine (5 mmol) in dichloromethane (20 mL) was added 2.2 equiv of triethylamine, followed by 1 equiv of benzoyl chloride, or 0.5 equiv of isophthaloyl dichloride, or 0.33 equiv of 1,3,5-benzenetricarbonyl trichloride in dichloromethane (10 mL). After the mixture was stirred for 10 min, the solvent was removed using a rotary evaporator. The solid residue was washed with water and recrystallized from DMF: water. The resulting crystalline amide was washed with water and dried under vacuum.

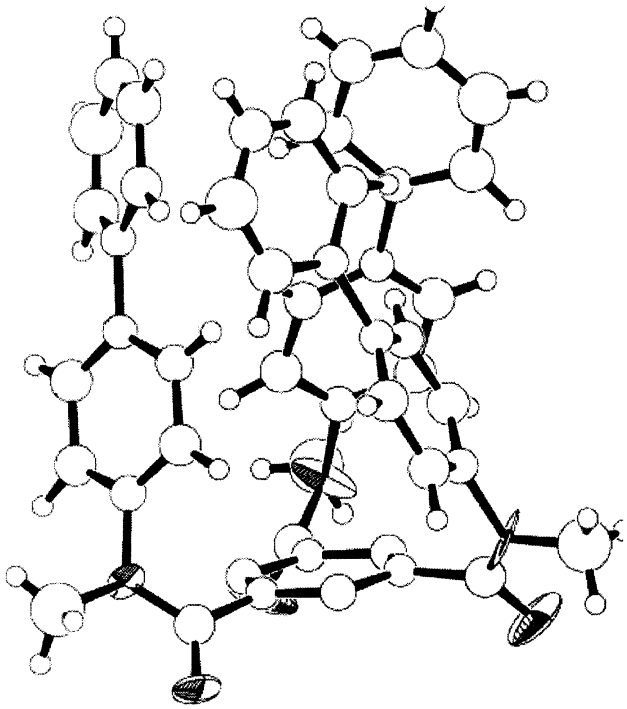

Figure 1. ORTEP representation of **3BP3**.

*N,N′-Diphenyl-1,3-benzenedicarboxamide (**2P2**).* mp 279−281 °C (lit.[15] mp 280 °C).

*N,N′,N″-Triphenyl-1,3,5-benzenetricarboxamide (**2P3**).* mp 326−328 °C (lit.[16] mp 327−329 °C).

*N-[1,1′-Biphenyl]-4-yl-benzamide (**2BP1**).* mp 232−234 °C (lit.[4] mp 233−234 °C). ^{1}H NMR (DMSO-d_6, 300 MHz): δ 7.34 (t, ^3J = 7.5 Hz, 1H), 7.46 (t, ^3J = 7.8 Hz, 2H), 7.48−7.63 (m, 3H), 7.68 (dm, ^3J = 8.7 Hz, 4H), 7.89 (dm, ^3J = 8.7 Hz, 2H), 7.98 (dm, ^3J = 7.2 Hz, 2H), 10.46 (s, 1H).

*N,N′-Bis[1,1′-biphenyl]-4-yl-1,3-benzenedicarboxamide (**2BP2**).* mp > 300 °C. ^{1}H NMR (DMSO-d_6, 300 MHz): δ 7.35(dd, ^3J = 7.5 Hz, 2H), 7.46 (t, ^3J = 7.5 Hz, 4H), 7.55 (d, ^3J = 7.2 Hz, 1H), 7.70 (t, ^3J = 6.6 Hz, 8H), 7.91 (t, ^3J = 8.4 Hz, 4H), 8.18 (dd, ^3J = 8.1 Hz, 2H), 8.58 (dd, ^3J = 8.4 Hz, 1H), 10.58 (s, 2H). MS *m/e* 468 ($M^{+\bullet}$).

*N,N′,N″-Tris[1,1′-biphenyl]-4-yl-1,3,5-benzenetricarboxamide (**2BP3**).* mp >360 °C. ^{1}H NMR (DMSO-d_6, 300 MHz): δ 7.35 (tt, ^3J = 7.5 Hz, 3H), 7.47 (t, ^3J = 7.5 Hz, 6H), 7.71 (d, ^3J = 9.3 Hz, 6H), 7.74 (d, ^3J = 8.1 Hz, 6H), 7.97 (d, ^3J = 8.7 Hz, 6H), 8.78 (s, 3H), 10.75 (s, 3H). MS *m/e* (%) 664 (MH^+, 95), 495(12), 307(100), 289(50).

*N-[4-(Phenylethynyl)phenyl]-benzamide (**2DPA1**).* mp 207−209 °C (lit.[4] mp 208−209 °C). ^{1}H NMR (DMSO-d_6, 300 MHz): δ 7.4−7.45 (m, 3H), 7.50−7.65 (m, 7H), 7.88 (dm, ^3J = 9 Hz, 2H), 7.96 (dm, ^3J = 7.5 Hz, 2H), 10.46 (s, 1H). MS *m/e* 297 ($M^{+\bullet}$).

*N,N′-Bis-[4-(phenylethynyl)phenyl]-1,3-benzenedicarboxamide (**2DPA2**).* mp >360 °C. ^{1}H NMR (DMSO-d_6, 300 MHz): δ 7.4−7.46 (m, 6H), 7.52−7.61 (m, 8H), 7.73 (t, ^3J = 7.2 Hz, 1H), 7.88−7.91 (m, 4H), 8.17 (dd, ^3J = 7.8 Hz, ^4J = 1.5 Hz, 2H), 8.54 (s, 1H), 10.63 (s, 2H). MS *m/e* 516 ($M^{+\bullet}$).

*N,N′,N″-Tris-[4-(phenylethynyl)phenyl]-1,3,5-benzenetricarboxamide (**2DPA3**).* mp > 360 °C. ^{1}H NMR (DMSO-d_6, 300 MHz): δ 7.42−7.44 (m, 9H), 7.54−7.58 (m, 6H), 7.60 (d, ^3J = 8.7 Hz, 6H), 7.92 (d, ^3J = 8.7 Hz, 6H), 8.74 (s, 3H), 10.80 (s, 3H). MS *m/e* 735 ($M^{+\bullet}$).

General Procedure for Preparing Tertiary Benzamides. A solution of NaH (10 mmol) in DMF (10 mL) was added

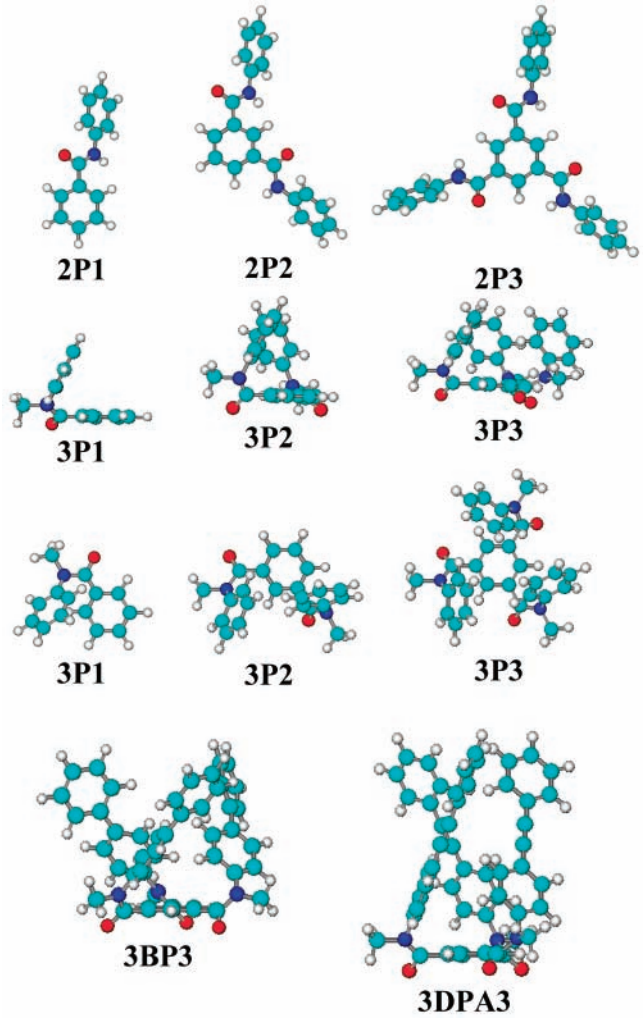

Figure 2. Optimized ground-state geometries for mono-, di-, and tribenzamides.

TABLE 1: Calculated Heats of Formation for Low-Energy Benzamide Conformations

monosubtituted amide	E_o, kcal/mol[a]	trans[b]	cis[b]
2P1	−2948.1	(0.0)	+2.7
2BP1	−4156.3	(0.0)	+3.0
2DPA1	−4447.6	(0.0)	+2.5
3P1	−3212.9	+1.9	(0.0)
3BP1	−4421.2	+1.9	(0.0)
3DPA1	−4712.8	+3.0	(0.0)

disubstituted amide	E_o, kcal/mol[a]	trans,trans	syn (cis,cis)	anti (cis,cis)
2P2	−4578.0	(0.0)	+5.0	+4.5
2BP2	−6994.7	(0.0)	+5.0	+6.1
3P2	−5109.5	+4.1	(0.0)	+0.1
3BP2	−7525.8	+5.1	(0.0)	+0.5

trisubstituted amide	E_o, kcal/mol[a]	all-trans	syn (all-cis)	anti (all-cis)
2P3	−6207.0	(0.0)	+6.5	6.3
2BP3	−9834.0	(0.0)	+8.8	+9.4
3P3	−7005.4	+6.2	(0.0)	−0.2
3BP3	−10630.3	+6.0	(0.0)	+0.7

[a] Heats of formation for low-energy conformers were obtained from AM1 calculations using Hyperchem, with geometry optimization by AM1 to RMS gradient of 0.1 kcal. [b] Energy of higher energy conformers relative to that of the lowest energy conformer (0.0).

dropwise to a solution of the secondary benzamides (0.6 equiv for monoamide, 0.3 equiv for diamides, and 0.2 equiv for triamides) in DMF (20 mL) in 20 min, during which 1.2 equiv of iodomethane was added. The mixture was stirred at room temperature and followed by TLC until the starting material was consumed (ca. 2−3 h), mixed with water (20 mL), and extracted with 20 mL CH_2Cl_2. The organic layer was washed with water (20 mL) three times and dried with anhydrous potassium carbonate (3 g). After the solvent was removed, the residue was purified by column chromatography using mixed solvents (acetone and hexane).

*N,N′-Dimethyl-N,N′-diphenyl-1,3-benzenedicarboxamide (**3P2**).* mp 165−166 °C (lit.[15] mp 164−166 °C)

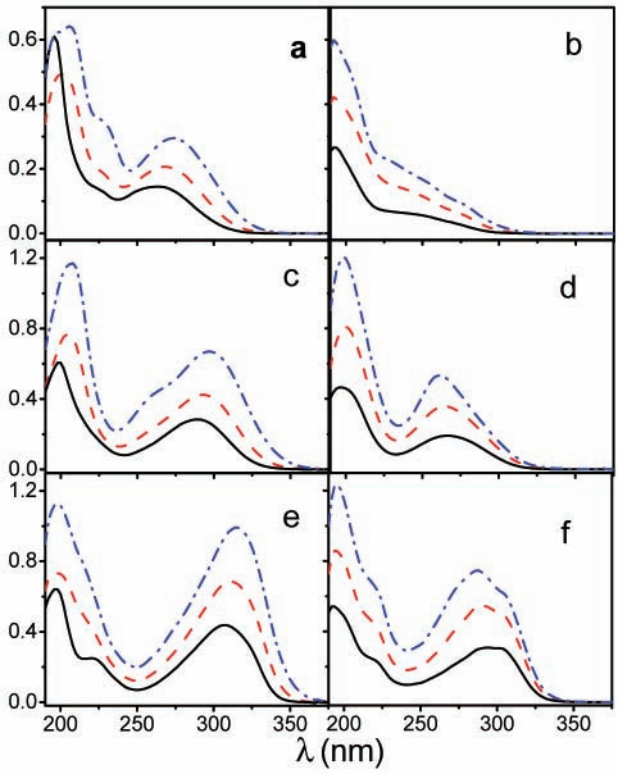

Figure 3. Absorption spectra of 10 mM benzamides in acetonitrile solution. (a) **2P1** (solid), **2P2** (dash), **2P3** (dash dot). (b) **3P1** (solid), **3P2** (dash), **3P3** (dash dot). (c) **2BP1** (solid), **2BP2** (dash), **2BP3** (dash dot). (d) **3BP1** (solid), **3BP2** (dash), **3BP3** (dash dot). (e) **2DPA1** (solid), **2DPA2** (dash), **2DPA3** (dash dot). (f) **3DPA1** (solid), **3DPA2** (dash), **3DPA3** (dash dot).

TABLE 2: UV Spectral Data for Benzamides in Acetonitrile Solution

amide	absorbance[a] λ_{max}, nm	absorbance[a] ϵ, M^{-1}	intensity ratio[b]
2P1	262	14500	(1.0)
2P2	268	20700	1.43
2P3	274	29500	2.0
3P1	250	5500	(1.0)
3P2	250	11400	2.16
3P3	250	16600	3.25
2BP1	290	28400	(1.0)
2BP2	294	42300	1.49
2BP3	298	66900	2.35
3BP1	266	19100	(1.0)
3BP2	264	35700	1.87
3BP3	262	53300	2.78
2DPA1	308	43700	(1.0)
2DPA2	312	68500	1.56
2DPA3	314	99100	2.26
3DPA1	294	30800	(1.0)
3DPA2	290	54800	1.78
3DPA3	288	74600	2.42

[a] Measured at room temperature. [b] Ratio of intensities of di- or triamides to monoamide (1.0).

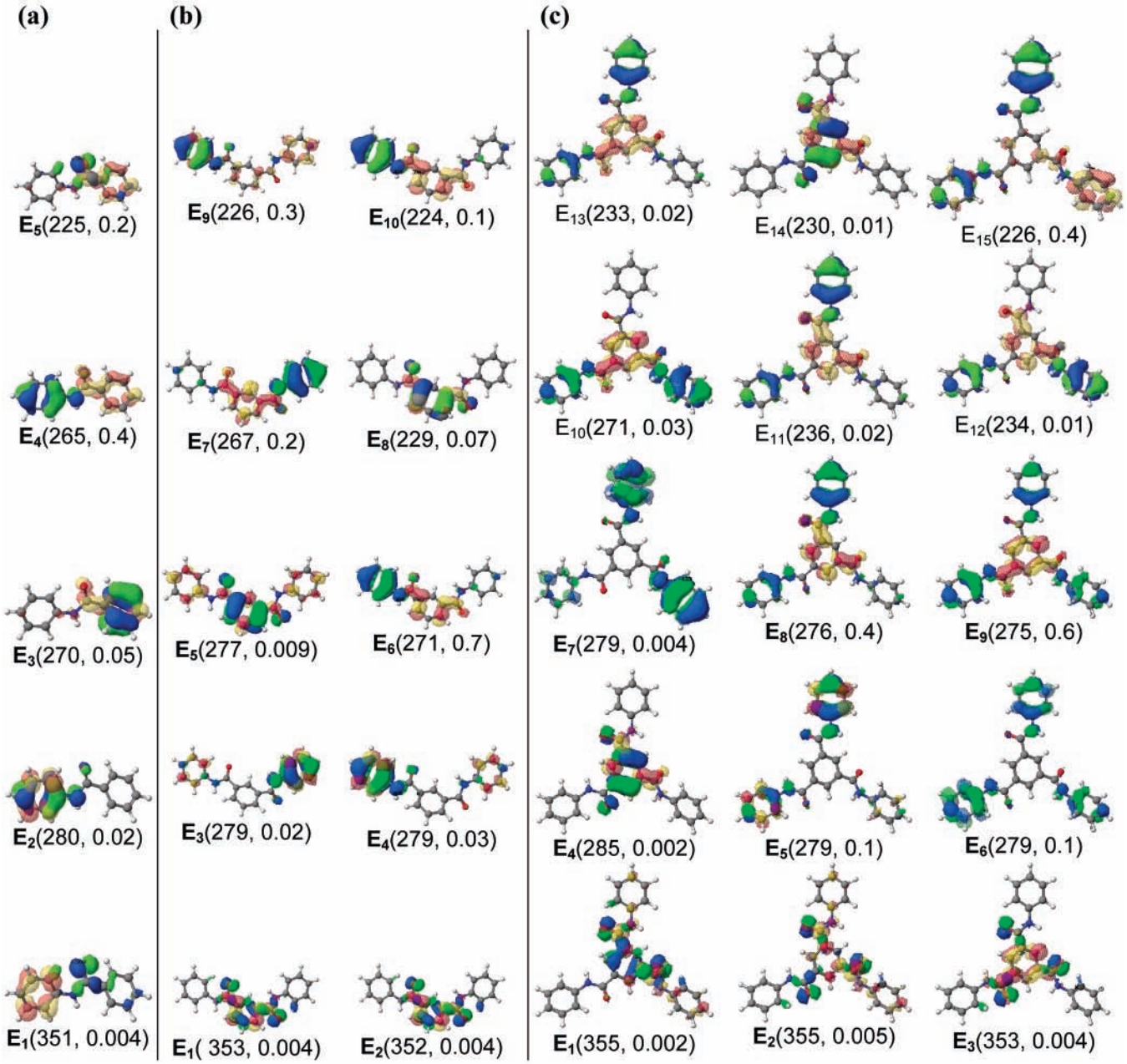

Figure 4. Energies, oscillator strengths, and dominant configurations for the lowest singlet−singlet transitions of (a) **2P1**, (b) **2P2**, and (c) **2P3**. Occupied orbitals shown in green and blue, unoccupied orbitals shown in red and yellow.

*N,N′,N″-Trimethyl-N,N′,N″-triphenyl-1,3,5-benzenetricarboxamide (**3P3**).* mp 262−263 °C (lit.[15] mp 262−263 °C).

*N-Methyl-N-[1,1′-biphenyl]-4-yl-benzamide (**3BP1**).* mp 117−119 °C. ^{1}H NMR ($CDCl_3$, 300 MHz): δ 3.55 (s, 3H), 7.09−7.12 (m, 2H), 7.17−7.27 (m, 3H), 7.34−7.38 (m, 3H), 7.39−7.48 (m, 4H), 7.51−7.55 (m, 2H). MS *m/e* (%) 288 (MH^+, 100), 221(8), 182(5).

*N,N′-Dimethyl-N,N′-bis[1,1′-biphenyl]-4-yl-1,3-benzenedicarboxamide (**3BP2**).* mp 216−218 °C. ^{1}H NMR ($CDCl_3$, 300 MHz): δ 3.46 (s, 6H), 6.93 (d, ^3J = 8.4 Hz, 4H), 6.96 (t, ^3J = 8.4 Hz, 1H), 7.16 (d, ^3J = 7.2 Hz, 2H), 7.34−7.48 (m, 15H). MS *m/e* (%) 497 (MH^+, 100), 314(20), 307(5), 289(5), 260-(10).

*N,N′,N″-Trimethyl-N,N′,N″-tris[1,1′-biphenyl]-4-yl-1,3,5-benzenetricarboxamide (**3BP3**).* mp > 300 °C. ^{1}H NMR ($CDCl_3$, 300 MHz): δ 3.38 (s, 9H), 6.46 (d, ^3J = 7.8 Hz, 6H), 6.98 (dm, ^3J = 7.5 Hz, 12H), 7.16 (s, 3H), 7.36−7.44 (m, 9H). MS *m/e* (%) 706 (M^+, 100), 555(20), 523(20).

*N-Methyl-N-[4-(Phenylethynyl)phenyl]benzamide (**3DPA1**).* mp 118−119 °C. ^{1}H NMR ($CDCl_3$, 300 MHz): δ 3.51 (s, 3H), 7.01 (d, ^3J = 8.7 Hz, 2H), 7.16−7.23 (m, 2H), 7.24−7.28 (m, 1H), 7.30−7.32 (m, 1H), 7.33−7.36 (m, 4H), 7.38 (d, ^3J = 8.7 Hz, 2H), 7.51 (d, ^3J = 10.5 Hz, 2H), 7.48−7.52 (m, 2H). MS *m/e* 309 ($M^{+\bullet}$).

*N,N′-Dimethyl-N,N′-bis-[4-(Phenylethynyl)phenyl]-1,3-benzenedicarboxamide (**3DPA2**).* mp 220−222 °C. ^{1}H NMR ($CDCl_3$, 300 MHz): δ 3.45 (s, 6H), 6.86 (dm, ^3J = 8.4 Hz, 4H), 7.0 (tm, ^3J = 8.4 Hz, 1H), 7.13−7.17 (m, 2H), 7.26−7.34 (m, 6H), 7.39 (t, ^4J = 1.5 Hz, 1H), 7.44 (d, ^3J = 8.7 Hz, 4H), 7.48−7.51 (m, 4H). MS *m/e* 544 ($M^{+\bullet}$).

*N,N′,N″-Trimethyl-N,N′,N″-tris-[4-(Phenylethynyl)phenyl]-1,3,5-benzene-tricarboxamide (**3DPA3**).* mp 293−294 °C. ^{1}H NMR ($CDCl_3$, 300 MHz): δ 3.38 (s, 9H), 6.58 (d, ^3J = 8.4 Hz, 6H), 7.14 (s, 3H), 7.16−7.34 (m, 9H), 7.48−7.52 (m, 6H), 7.54 (d, ^3J = 8.7 Hz, 6H). MS *m/e* 777 ($M^{+\bullet}$).

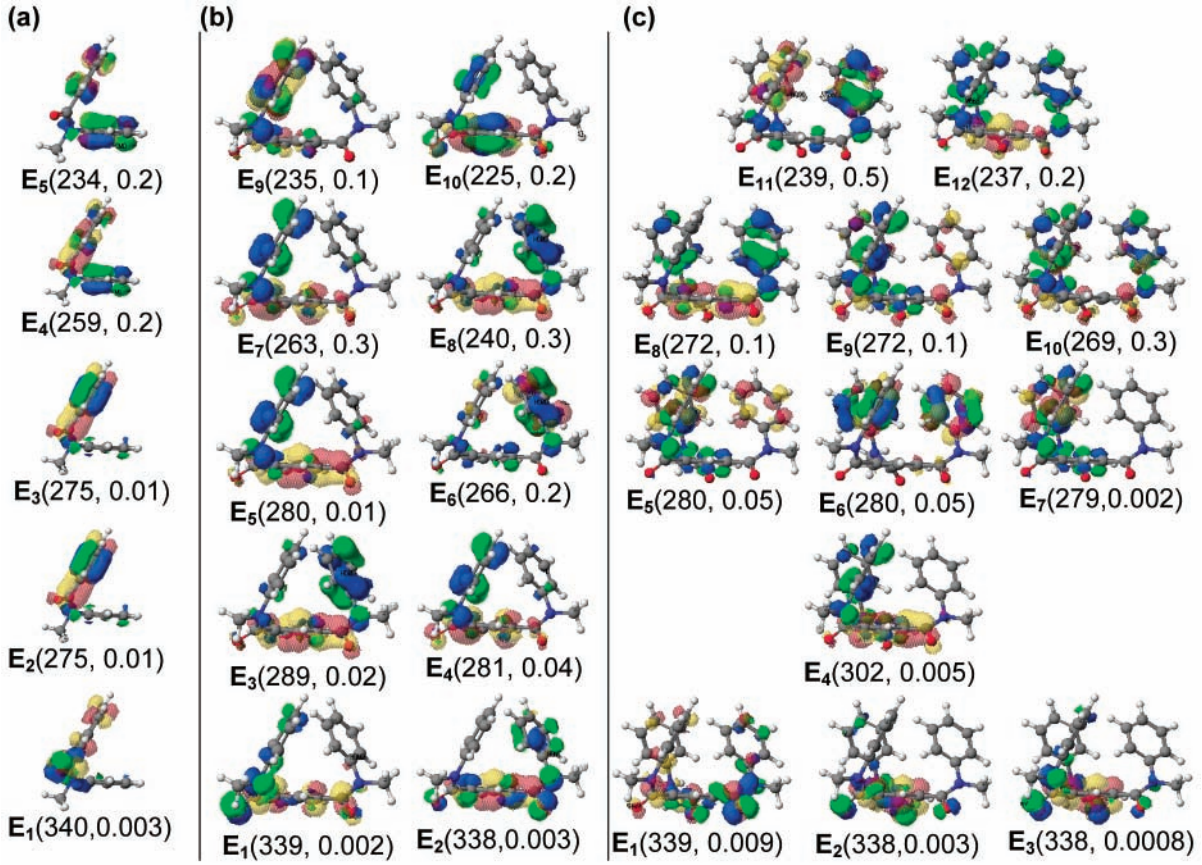

Figure 5. Energies, oscillator strengths, and dominant configurations for the lowest singlet−singlet transitions of (a) **3P1**, (b) **3P2**, and (c) **3P3**. See Figure 4 for color code.

Results and Discussion

Molecular Structure. The crystal structures of the secondary amides **2P1**, **2P2**, and **2P3** and those of the tertiary amides **3P1**, **3P2**, and **3P3** have been reported.[8] The secondary amides possess all-trans amide conformations, whereas the tertiary amides possess all-cis conformations. The crystal structure of **3BP3** has been determined and found to belong to the space group *P*3(no. 143). Each of the three molecules in the unit cell has an all-cis conformation in which all three biphenyl groups reside on the same side of the benzenetricarboxamide ring, but have slightly different geometries (Figure 1). The three biphenyls are nonplanar, with phenyl−phenyl torsion angles of 22, 31, and 32°. The parent biphenyl molecule has a torsion angle of 35° in solution.[17] Both twisted and planar structures have been reported for biphenyl in solid phases, the torsion angle being determined by crystal packing forces. The three biphenyls in **3BP3** adopt an edge-to-face arrangement, similar to that observed for adjacent molecules in a one-dimensional tape of *N*,*N*-dimethyl-1,4′-biphenyldicarboxamide.[18]

The AM1-minimized structures of the secondary amides **2P1**, **2P2**, and **2P3** and those of the tertiary amides **3P1**, **3P2**, and **3P3** are shown in Figure 2 along with the all-syn structures of **3BP3** and **3DPA3**. The calculated structure for **3BP3** is similar to the crystal structure. The crystal structure and AM1 minimized structures of **2P1** and **3P1** have previously been compared.[5] In the crystal structure, the dihedral angle between phenyl rings is ca. 30° as a consequence of twisting about the phenyl−CO and phenyl−NH bonds. The calculated potential energy surface for twisting about these bonds is very shallow, the energy of the fully planar structure differing from that of the nonplanar structure by <1 kcal/mol. The experimental and calculated twist angles for **3P1** are larger than those for **2P1**.

The calculated heats of formation for the AM1-minimized conformations of most of the amides are summarized in Table 1. For the secondary amides, the trans amide conformations are more stable than the cis by a minimum of 2.5 kcal/mol. Conversely, for the tertiary amides the cis conformations are more stable than the trans by a minimum of 1.9 kcal/mol. For the tertiary di- and triamides the calculated heats of formation for the syn and anti conformations of **3P2** and **3P3** are similar, in accord with the observation of fast NMR exchange of the syn and anti rotamer of **3P3**.[8] However, the syn conformations of **3BP2** and **3BP3** are calculated to be more stable than the anti conformers by ca. 0.5 kcal/mol.

Experimental evidence for a syn-conformer preference for the tertiary di- and triamides of **BP** and **DPA** is provided by analysis of their NMR spectra. The protons adjacent to the nitrogens appear as a readily identified doublet, which moves upfield with the introduction of successive amide substituents as a consequence of aryl−aryl shielding. For example, the shifts of these protons for **3BP1, 3BP2**, and **3BP3** are at 7.10, 6.93, and 6.46, respectively. Similar results are obtained for the tertiary **DPA**-containing amides. The larger upfield shift for the tri- vs diamide is consistent with an all-syn conformation rather than a syn−anti conformation for both **3BP3** and **3DPA3**. The larger preference for the all-syn conformation of these amides vs **3P3** can be attributed to more extensive edge-to-face interactions in the larger arenes.[19]

Electronic Absorption Spectra. The absorption spectra of the 18 benzamides are shown in Figure 3. All of the spectra display a short wavelength band near 200 nm and a single long-wavelength band. The position and molar absorbance of the long-wavelength maxima are reported in Table 2. In the case of the tertiary **3P(*n*)** series, the long-wavelength band is not

resolved and the absorbance at 250 nm is reported. In the case of the secondary amides, increasing the number of amide groups results in a red shift in the absorption maxima (Figure 3a,c,e). The absorbance ratios for the secondary mono-, di-, and triamides are approximately 1:1.5:2.2. In the case of the tertiary amides of **BP** and **DPA**, increasing the number of amide groups results in a blue shift in the absorption maximum (Figure 3d,f). The absorbance ratios for the tertiary mono-, di-, and triamides are approximately 1:2:3. In the case of the **2BP(*n*)**, **2DPA(*n*)**, and **3BP(*n*)** families there is also distinct change in band shape with increasing substitution, the bands appearing to "lean" in the direction of the band maximum.

The modest red shifts for the families of secondary amides are similar to those reported for biphenyl, *m*-terphenyl, and 1,3,5-triphenylbenzene.[9] However, this series displays a more pronounced increase in oscillator strength for the long-wavelength absorption band (1:2.9:3.6) than is observed for the secondary amides. The fluorescence maxima undergo a pronounced red shift accompanied by an increase in singlet lifetime. Evidently the singlet state is delocalized, unlike the long-wavelength transitions in the absorption spectra, which are proposed to be localized on the individual biphenyl units.[9]

ZINDO Calculations. We have previously employed semiemperical INDO/S SCF-CI (ZINDO) calculations using the algorithm developed by Zerner and co-workers[20] to investigate the electronic transitions of **2P1**, **2BP1**, **2DPA1**, and **3P1**.[4,5] ZINDO calculations have been conducted for all 18 amides using their AM1-minimized geometries. The results of these calculations are shown in Figure 4 for the **2P(*n*)** family, in Figure 5 for the **3P(*n*)** family, and in Figure 6 for **3BP3**. The use of color coding (blue and green for occupied orbitals and yellow and red for unoccupied orbitals) facilitates visualization of the dominant configuration for each of the transitions. The calculated wavelength and oscillator strength for each transition are also reported in the figures.

The lowest energy transition for all 18 amides is a forbidden n,π* benzoyl-localized (n,B*) state, which accounts for the fluorescence behavior of these molecules (vide infra). The lowest energy allowed transitions for the **2P(*n*)** family are E_4, $E_{6,7}$, and $E_{8,9}$, for $n = 1$, 2, and 3, respectively (Figure 3). All of these are π,π* transitions of aniline,benzoyl (A,B*) character. Their maxima are slightly red-shifted with increasing substitution, as are the observed spectra (Figure 4a). The lowest energy allowed transitions for the **3P(*n*)** family are E_4, $E_{6,7,8}$, and $E_{10,11}$, for $n = 1$, 2, and 3, respectively. Most of these transitions can also be described as A,B* transitions in which the occupied orbital is localized on a single aniline ring. The increase in calculated oscillator strength near 340 nm with increasing substitution is consistent with the appearance of the spectra (Figure 3b).

The transitions for one of the more complex structures, **3BP3**, are shown in Figure 6. The lowest energy states correspond to three forbidden n,B* transitions originating in the three different carbonyl n-orbitals. The lowest energy allowed transitions are $E_{9,13,14}$ (A,B*) and E_{15} (A,A*). The A,A* transitions $E_{5,6,7}$ are localized on a singlet biphenyl and have low oscillator strengths, as does the lowest energy transition of the parent biphenyl molecule.[17] Transitions $E_{10,11,12}$ display coupling between two biphenyls, but also have low oscillator strengths.

Excitonic interaction between biphenyl-localized transitions provides a possible explanation for the blue-shifted absorption maximum for the **3BP(*n*)** and **3DPA(*n*)** families (Figure 3d,f) and the red-shifted absorption for the **2BP(*n*)** and **2DPA(*n*)** families with increasing *n* (Figure 3b). Exciton splitting between

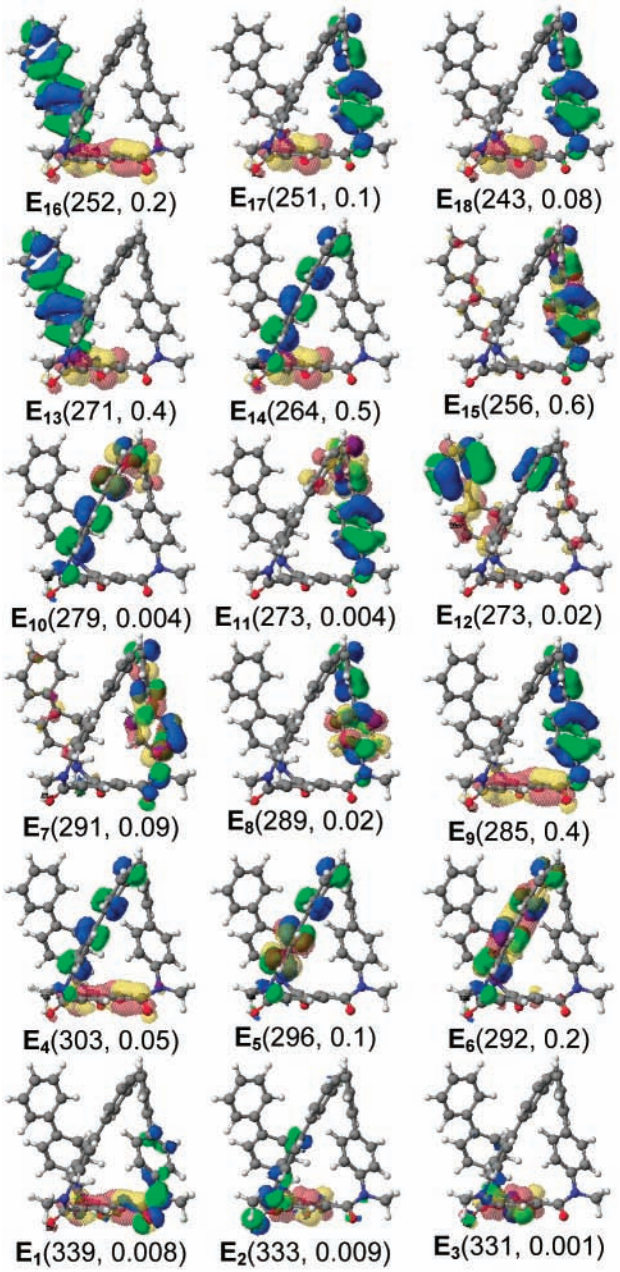

Figure 6. Energies, oscillator strengths, and dominant configurations for the lowest singlet−singlet transitions of **3BP3**. See Figure 4 for color code.

parallel biphenyl chromophores (H-aggretate structure) in **3BP2** and **3BP3** should result in a weak long wavelength band and a strong short wavelength band.[21] In contrast, exciton splitting between the biphenyls in **2BP2** and **2BP3**, which have aligned vector components (J-aggregate structure), should result in a strong long wavelength band and a weak short wavelength band. The strength of the exciton splitting shows a $1/R^3$ dependence upon the distance between chromophores and hence should be larger for the tertiary versus secondary amides.[21] This may account for the larger gain in molar absorbance for the tertiary versus secondary amides with increasing substitution (Table 2).

The ability of the ZINDO calculations to replicate the observed absorption spectra is illustrated in Figures 7 and 8. Figure 7 shows the calculated spectrum of **2P1** obtained with no band broadening (vectors) and using three different peak widths. The maxima at 265 and 240 nm correspond to transitions E_4 and E_5 in Figure 4, while the maximum at 200 nm

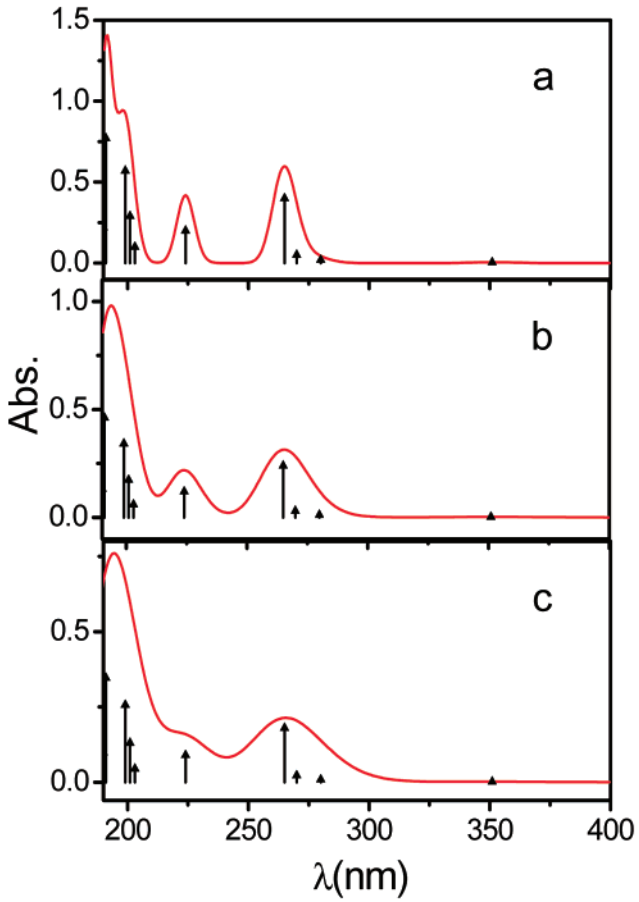

Figure 7. Calculated absorption spectra for **2P1** with bandwidths of (a) 1600 cm^{-1}, (b) 3200 cm^{-1}, and (c) 4800 cm^{-1}. Vectors indicate calculated energies and oscillator strengths of singlet transitions. Tailless vectors have very low oscillator strengths.

corresponds to higher energy transitions. Figure 8 compares the observed spectra for **2P1**, **3P3**, and **3BP3** with spectra calculated using peak widths of 4800 cm^{-1}. The agreement is excellent for all three amides. Whereas we have used all of the ZINDO-calculated transitions to simulate the absorption spectrum, the fits are dominated by a small number of individual or degenerate transitions and thus can be reproduced using three arbitrary Gaussian functions. Substantial band broadening is necessary in order to replicate the observed spectra. The band broadening presumably is a consequence of several factors, including shallow ground-state potential energy minima with underlying vibrational progressions.

The ZINDO calculations also appear to replicate the excitonic interactions between arene groups. For example, transitions E_6 and E_7 of **2P2** and transitions E_8 and E_{11} of **2P3** (Figure 4) have the same symmetries but different energies. The lower energy transition possesses the greater oscillator strength, as expected for an J-aggregate. In the case of the tertiary amide **3BP3**, transitions E_4 and E_9 have the same symmetries but different energies. The higher energy transition possesses the greater oscillator, as expected for an H-aggregate. There is precedent for the ability of ZINDO calculations to replicate aggregate spectra. ZINDO/S calculations for clusters of four quaterthiophene molecules in an H-aggregate structure reproduce the absorption spectral shifts observed in thin films, which presumably exist as larger aggregates, when compared to the isolated molecules in solution.[22]

The lowest triplet states of all 18 amides were also calculated using ZINDO, as previously reported for the secondary amides

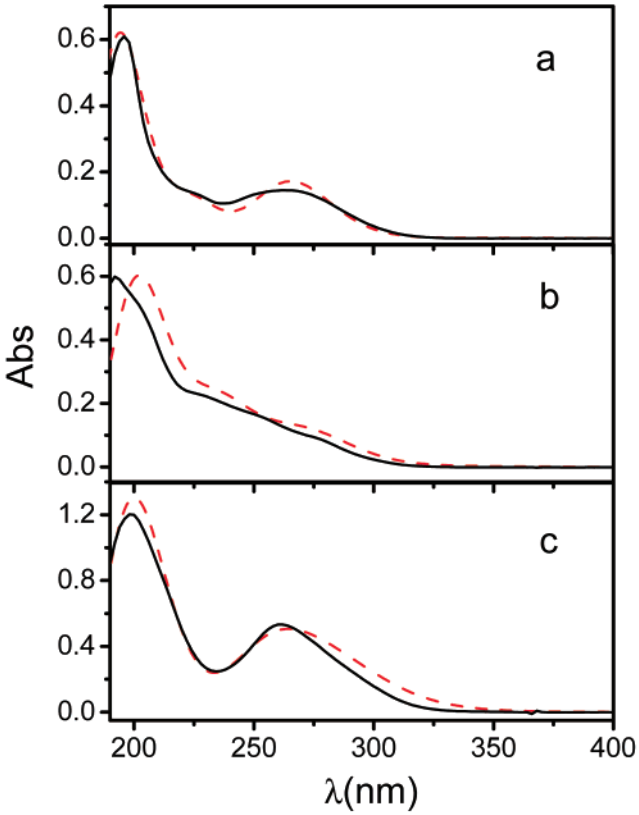

Figure 8. Comparison of experimental (solid) and calculated (dash) absorption spectra of (a) **2P1**, (b) **3P3**, and (c) **3BP3**.

2P1, **2BP1**, and **2DPA1**.[4] The two singly occupied molecular orbitals ($SOMO_1$ and $SOMO_2$) for the **2P(*n*)** and **3P(*n*)** families and those for **2BP1** are shown in Figure 9. In the case of **2P1** both SOMOs are largely localized on the anilide portion of the molecule. Delocalization into the benzoyl portion is observed to increase with increasing amide substitution for **2P2** and **2P3**. Both SOMOs are delocalized for all three members of the **3P-(*n*)** family. For all of the other secondary and tertiary amines, both SOMOs are largely localized on a single *N*-aryl substituent, as shown for **2BP1** in Figure 9. The character of the triplet state will be seen to influence the phosphorescence behavior (vide infra).

Luminescence Spectra. All 18 amides display overlapping fluorescence and phosphorescence at 77 K in MTHF glass. Wavelengths, decay times, and quantum yields are summarized in Table 2 along with data for the parent arylamines. Representative time-resolved fluorescence and phosphorescence spectra are shown in Figure 10. Broad structureless fluorescence is observed in all cases. The phosphorescence of the benzanilides is also structureless; however, the phosphorescence of the amides possessing **BP** or **DPA** is structured and similar in appearance to that of the parent arylamines, as previously reported for **2BP1** and **2DPA1**.[4]

The fluorescence of **2P1** and **3P1** has been the subject of several investigations and some controversy.[3,7,23] We recently reported the results of an experimental and computational study of the luminescence and excited-state potential energy surfaces for these benzanilides.[5] Both display very weak room-temperature fluorescence with large Stokes shifts ($\lambda_{max} = 475$ nm) in nonpolar solvents. This emission is assigned to an intramolecular charge transfer state which is twisted about the amide C−N bond, in agreement with the assignment of Azumaya et al.[7] The emission maximum of **2P1** in MTHF glass at 77 K occurs at shorter wavelength (Table 3), as a consequence of restricted

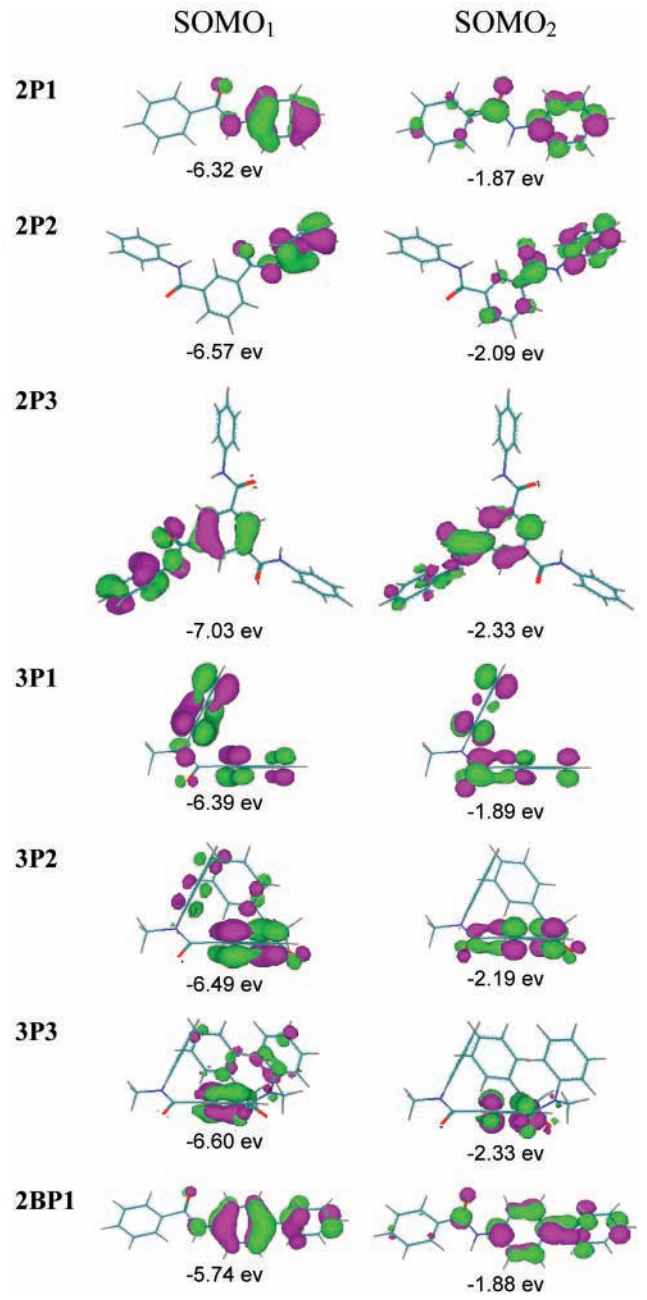

Figure 9. Singly occupied orbitals for the triplet states of **2P(*n*)**, **3P-(*n*)**, and **2BP1**.

C−N rotation. The emission maxima of the highly nonplanar amide **3P1** are similar in solution and at 77 K and are attributed to the twisted n,B* singlet state.

The 77 K fluorescence spectra of all of the secondary amides are similar in appearance and are attributed to the planar n,B* lowest singlet state. This assignment is consistent with the results of ZINDO calculations showing that the n,B* states for all of the secondary amides have similar energies ($\lambda_{max} = 430 \pm 10$ nm) and lie well below the allowed π,π^* transitions. They also have similar singlet lifetimes (2−4 ns) and moderately large fluorescence quantum yields (Table 3). The fluorescence spectra of all of the tertiary amides resemble that of **3P1** and are attributed to the nonplanar n,B* singlet state. Their fluorescence maxima are similar (500 ± 10 nm, except in the case of **3P3**). Their singlet decay times are also similar (2.5−4.7 ns), and their fluorescence quantum yields are distinctly smaller than those of the secondary amides.

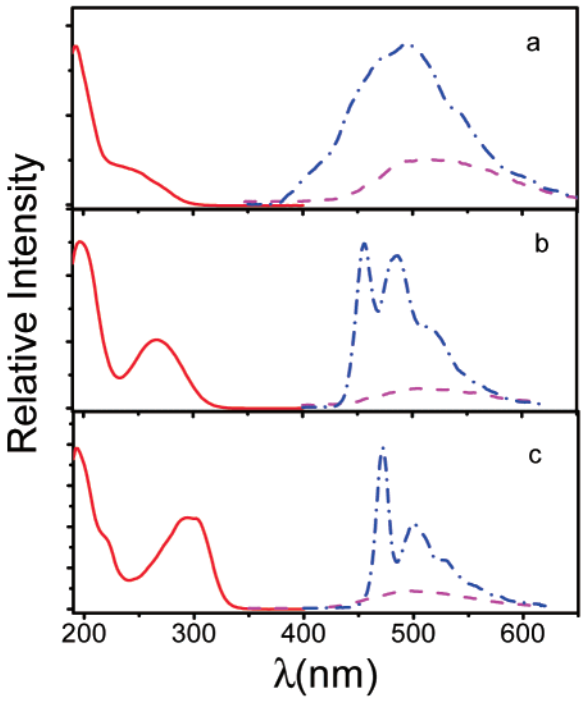

Figure 10. Absorption (solid), fluorescence (dash), and phosphorescence (dash dot) spectra of (a) **3P1**, (b) **3BP1**, and (c) **3DPA1**.

TABLE 3: Low-Temperature Emission Spectra Data for Benzamides in MTHFat 77 K

	fluorescence			phosphorescence		
amine or amide[a]	λ_{max}, nm	t_s, ns	Φ_f	λ_{max}, nm	t_t, s	Φ_p
PhNH$_2$	325	1.92	0.23	405	4.42	0.45
2P1	430	3.63	0.25	410	0.4	0.37
2P2	430	3.50	0.24	420	0.17	0.10
2P3	430	3.02	0.16	430	0.08	0.03
3P1	510	2.52	0.01	460	0.0017	0.01
3P2	490	*b*	0.01	430	0.0009	0.01
3P3	470	3.00	0.04	430	0.0033	0.04
BpNH$_2$	365	10.65	0.61	470	3.52	0.07
2BP1	420	3.97	0.45	460	2.0	0.07
2BP2	430	3.34	0.27	460	1.78	0.03
2BP3	440	3.04	0.26	460	1.45	0.02
3BP1	510	3.30	0.05	460	1.76	0.20
3BP2	510	3.91	0.03	455	1.8	0.14
3BP3	510	3.32	0.02	450	1.98	0.10
DPANH$_2$	360	1.25	0.33	480	1.57	0.02
2DPA1	420	2.06	0.44	470	0.747	0.02
2DPA2	425	3.15	0.39	475	0.655	0.01
2DPA3	430	2.67	0.29	480	0.644	0.07
3DPA1	500	3.43	0.06	470	0.675	0.07
3DPA2	500	4.73	0.05	470	0.634	0.05
3DPA3	500	4.35	0.05	470	0.609	0.05

[a] Data for amines from ref 4. [b] Lifetime not measured.

The phosphorescence spectra of all of the secondary and tertiary **BP** and **DPA** amides display structure and decay times similar to those of the parent arylamines.[4] This observation is consistent with the results of ZINDO calculations (Figure 9) which indicate that both SOMOs of the triplet state are localized on the arylamine. This is not the case for the secondary and tertiary anilides, all of which have red-shifted emission maxima and shorter fluorescence decay times than aniline. The ZINDO calculations for the triplet states indicate that the SOMOs of all of the **3P(*n*)** amides are extensively delocalized. Mixing of n,π^* character in the case of these amides should reduce their triplet lifetimes compared to that of aniline, as is observed. In the case of the **2P(*n*)** family, delocalization increases as *n*

increases, providing a plausible explanation for the decrease in triplet lifetime and quantum yield.

Concluding Remarks. The conformational preferences of the secondary and tertiary benzamides possessing **BP** or **DPA** groups are similar to those previously reported for the corresponding secondary and tertiary anilides. All of the secondary benzamides have trans-amide conformations, resulting in extended geometries. In contrast, the tertiary benzamides have cis-amide conformations, resulting in folded geometries. The aryl groups of the di- and trisubstituted tertiary benzamides of **BP** and **DPA** occupy the same face of the benzamide ring. This syn preference is attributed to attractive edge-to-face interactions between the aryl groups.[19]

The absorption spectra of the secondary amides display a red shift with increasing substitution, whereas the spectra of the tertiary amides display a blue shift. Exciton splitting between transitions localized on the individual **BP** or **DPA** groups may be responsible for these shifts. Analysis of the electronic spectra using ZINDO calculations indicates that the lowest singlet state for all of the amides arises from a forbidden n,B* transition and that the lowest energy allowed transitions are of A,B* or A,A* character. All of the amides are very weakly fluorescent at room temperature. At 77 K in a MTHF glass the secondary and tertiary amides display structureless fluorescence attributed to planar and nonplanar n,B* states. The structured phosphorescence of both secondary and tertiary amides possessing **BP** and **DPA** groups is attributed to arene-localized A,A* transitions.

Acknowledgment. Financial support for this research has been provided by the National Science Foundation.

Supporting Information Available: X-ray crystallographic data for the tertiary amide **3BP3**. This material is available free of charge via the Internet at http://pubs.acs.org.

References and Notes

(1) Itai, A.; Toriumi, Y.; Tomioka, N.; Kagechika, H.; Azumaya, I.; Shudo, K. *Tetrahedron Lett.* **1989**, *30*, 6177−6180.
(2) Itai, A.; Toriumi, Y.; Saito, S.; Kagechika, H.; Shudo, K. *J. Am. Chem. Soc*. **1992**, *114*, 10649−14650.
(3) Lewis, F. D.; Long, T. M. *J. Phys. Chem. A* **1999**, *102*, 5327−5332.
(4) Lewis, F. D.; Liu, W.-Z. *J. Phys. Chem. A*, **1999**, *103*, 9678−9686.
(5) Lewis, F. D.; Liu, W.-Z. *J. Phys. Chem. A*, **2002**, *106*, 1976−1984.
(6) Yamaguchi, K.; Matsumura, G.; Kagechika, H.; Azumaya, I.; Ito, Y.; Itai, A.; Shudo, K. *J. Am. Chem. Soc*. **1991**, *113*, 5474−5475.
(7) Azumaya, I.; Kagechika, H.; Fujiwara, Y.; Itoh, M.; Yamaguchi, K.; Shudo, K. *J. Am. Chem. Soc*. **1991**, *113*, 2833−2838.
(8) Azumaya, I.; Kagechika, H.; Yamaguchi, K.; Shudo, K. *Tetrahedron*, **1995**, *51*, 5277−5290.
(9) Nijegorodov, N. I.; Downey, W. S.; Danailov, M. B. *Spectrochem. Acta A* **2000**, *56*, 783−795.
(10) Schmidt, B.; Rinke, M.; Güsten, H. *J. Photochem. Photobiol. A* **1989**, *49*, 131−135.
(11) Verbeek, G.; Depaemelaere, S.; Van der Auweraer, M.; De Schryver, F. C.; Vaes, A. Terrell, D.; De Meutter, S. *Chem. Phys.* **1993**, *176*, 195−213.
(12) Results for several of the monobenzamides have previously been reported.[4,5]
(13) Li, R.; Lim, E. C. *J. Chem. Phys.* **1972**, *57*, 605−612.
(14) James, D. R.; Siemiarczuk, A.; Ware, W. R. *Rev. Sci. Instrum.* **1992**, *63*, 1710−1716.
(15) Grimmel, H. W.; Guenther, A.; Morgan, J. F. *J. Am. Chem. Soc*. **1946**, *68*, 539−542.
(16) Palmans, A. R. A.; Vekemans, J. A. J. M.; Fischer, H.; Hikmet, R. A.; Meijer, E. W. *Chem. Eur. J*. **1997**, *3*, 300−307.
(17) Rubio, M.; Merchán, M.; Ortí, E.; Roos, B. O. *Chem. Phys. Lett.* **1995**, *234*, 373−381.
(18) Lewis, F. D.; Yang, J.-S.; Stern, C. L. *J. Am. Chem. Soc*. **1996**, *118*, 12029−12037.
(19) Jorgensen, W. L.; Severance, D. L. *J. Am. Chem. Soc.* **1990**, *112*, 4768−4774.
(20) Zerner, M. C.; Loew, G. H.; Kirchner, R. F.; Mueller-Westerhoff, U. T. *J. Am. Chem. Soc.* **1980**, *102*, 589.
(21) Cantor, C. R.; Schimmel, P. R. *Biophysical Chemistry*, *Part II*; W. H. Freeman: New York, 1980; p 395.
(22) DiCesare, N.; Belletete, M.; Garcia, E. R.; Leclerc, M.; Durocher, G. *J. Phys. Chem. A* **1999**, *103*, 3864−3875.
(23) Heldt, J.; Gormin, D.; Kasha, M. *J. Am. Chem. Soc*. **1988**, *110*, 8255−8256.